ISSN 1995-4212, Polymer Science, Series D, 2018, Vol. 11, No. 2, pp. 191–196. © Pleiades Publishing, Ltd., 2018.
Original Russian Text © L.E. Tsygankova, A.A. Zvereva, N. Al'shika, Yu.V. Gavrilov, O.V. Alekhina, 2017, published in Vse Materialy, 2017, No. 11, pp. 31–38.

Accumulation of Electrolytic Hydrogen by Carbon Nanotubes

L. E. Tsygankova[a], *, A. A. Zvereva[a], N. Al'shika[a], Yu. V. Gavrilov[b], and O. V. Alekhina[a]

[a] *Derzhavin Tambov State University, Tambov, 392000 Russia*
[b] *Mendeleev University of Chemical Technology of Russia, Moscow, 125047 Russia*
**e-mail: vits21@mail.ru*

Received March 22, 2017

Abstract—The accumulation of electrolytic hydrogen synthesized in a 5 M KOH solution by double- and triple-walled carbon nanotubes (CNTs) deposited on a steel membrane and encapsulated by an electrolytic iron layer of the thickness of 10 nm was studied. CNTs were synthesized by catalytic pyrolysis of methane and are characterized by an inner diameter of 2–4 nm, a length of up to 10 μm and more, and a specific surface area of 600–800 $m^2 g^{-1}$. The studies were performed by electrochemical diffusion, cyclic voltamperometry, and electrochemical-impedance spectroscopy. It has been shown that the hydrogen-storage capacity in CNTs varies in the range of 4–25% depending on the content of nanotubes in the composite.

Keywords: nanotubes, hydrogen, accumulation, storage capacity, diffusion, absorption, impedance, voltamperometry

DOI: 10.1134/S199542121802020X

The accumulation of hydrogen synthesized by different methods is one of the most serious problems of hydrogen power engineering. The existing methods for the hydrogen accumulation are either insufficiently efficient in terms of specific capacity or insufficiently manufacturable for practical use. These disadvantages are typical to varying degrees for hydride, liquid, compression, and sorption accumulation methods at decreased temperatures [1–3].

The manufacturability and the specific hydrogen-capacity requirements for accumulators of this kind can only increase with time. As far as can be determined from the results of foreign studies (United States, China, Japan, etc.), the aforementioned is also typical for the use of carbon nanotubes (CNTs) in such processes. Immediately after the discovery of CNTs in 1991 [4], their ability to store hydrogen attracted much attention. With the development of methods for the synthesis of carbon nanostructured materials, they become increasingly promising as hydrogen accumulators.

There are two known types of experimental methods for hydrogen uptake of CNTs. The first is the high-pressure method, which leads to the physical sorption of hydrogen molecules H_2 between clusters of the intertube space. The maximum hydrogen-storage capacity achieved under these conditions varies from 3 to 6%.

The other method is electrochemical hydrogen uptake of CNTs: in the electrochemical process, under normal pressure, atomic hydrogen H is released on the CNTs' surfaces or on composites containing CNTs and adsorbed to diffuse into the depth of nanotubes.

In the case of hydrogen accumulation by CNTs or electrode materials with their participation, cathodically synthesized hydrogen is simultaneously an adsorbate (the charge phase) and the participant of the anodic reaction (the discharge phase). Thus, it is important to relate these processes with the hydrogen-release reaction (HRR) kinetics and the presence of surface-oxide formations, which are typical for all carbon materials. Electrochemical methods make it possible to effectively control the degree of filling of the surface with the aforesaid oxide formations by cathodic and anodic polarization of CNTs or carbon composites containing them.

In [5], the hydrogen accumulation by the composite of single-walled carbon nanotubes (SWCNTs) on a palladium substrate encapsulated by thin palladium layers under electrolytic hydrogen uptake was studied. It was shown that SWCNTs increase the hydrogen capacity of the Pd–SWCNTs composite by 24–26% under electrolytic hydrogen uptake compared to pure Pd. The capacity of SWCNTs in the composite depends on the Pd–SWCNTs volume ratio and reaches 12% at $V(\mathrm{Pd})/V(\mathrm{SWCNT}) > 10$.

Previously [6], the effect of the cathodic polarization value, type of electrolyte, and its composition on hydrogen accumulation by multiwalled carbon nanotubes was studied. It was shown that, in an acidic medium (x M HCl + $(1 - x)$ M LiCl), the content of hydrogen absorbed by carbon nanotubes encapsulated on a steel membrane by an electrolytically precipitated

iron layer is 3–13.8 wt %. In an alkaline medium (1 M KOH), the absorbed-hydrogen fraction is 3.5–15 wt % and depends on the cathodic-polarization value (up to 0.4 V) and the weight of multiwalled carbon nanotubes.

In [7], the accumulation of electrolytic hydrogen by multiwalled carbon nanotubes (MWCNTs) was studied in a 5 M KOH solution by electrochemical methods. MWCNTs were deposited on a steel membrane and encapsulated by an electrolytic nickel layer of the thickness of 10 nm. The hydrogen-storage capacity of MWCNTs, according to the electrochemical-diffusion method, varies in the range of 4.6–6.5% depending on the amount of nanotubes.

The aim of this work is to study electrolytic hydrogen absorption by double- and triple-walled carbon nanotubes in an alkaline medium by electrochemical diffusion (solid-phase hydrogen flow through a membrane), voltamperometry, and impedance spectroscopy.

Double- and triple-walled CNTs were synthesized by catalytic pyrolysis of methane at the temperature of 930°C on a catalyst of the following composition: $[Co_{0.25}Mo_{0.75}]_{0.05}Mg_{0.95}O$. The synthesized CNTs, immediately after the synthesis, were exposed to the hydrochloric acid treatment for 10 h to eliminate the catalyst with the subsequent annealing in a CO_2 atmosphere at 920°C to eliminate carbon admixtures. The inner diameter of CNTs is 2–4 nm, the length is up to 10 μm and more, and the specific surface area is about 600–800 $m^2 g^{-1}$. The carbon product contains 60% of double- and triple-walled CNTs, the rest are tubes with less and more layers.

The electrochemical-diffusion method consists in the use of a cell of Devanathan cell type with a vertical 08PS steel membrane with a thickness of 300 μm and a surface area of 3.63 cm^2 separating the polarization and the diffusion compartment of a cell. One side of a membrane was coated with a certain volume of an aqueous–ethanol CNTs solution modified polyvinylpyrrolidone (PVP). A PVP additive was introduced to provide solution stability (to prevent the nanotubes from settling).

After the evaporation of the liquid phase, for increasing the adhesion of nanotubes to the membrane surface, the electrolytic precipitation of an iron layer of the thickness of 10 nm from a standard ironing electrolyte containing $FeSO_4$, $MgSO_4$, and H_2SO_4 was performed under the current density of 0.1 A/dm^2. The coating thickness was calculated based on the amount of passed electricity. A membrane prepared using this technique was placed in a Devanathan cell. Its cathodically polarizable side with deposited CNTs was in contact with the working electrolyte solution (5 M KOH), and the diffusion side was in contact with a titrated $KMnO_4$ solution. Atomic hydrogen adsorbed on the polarizable-membrane surface formed in accordance with the reaction

$$H_2O + e \rightarrow H_{ads} + OH^-, \quad (1)$$

partially recombines (molizes) with the formation of molecular hydrogen H_2, which transits into the gas phase. The second part is absorbed by nanotubes. The third part diffuses through a membrane in a permanganate solution, where is oxidizes.

Based on the change in the $KMnO_4$ solution's concentration, the amount of hydrogen diffused through a membrane is calculated. The similar experiment without CNTs was performed using a steel membrane coated with an electrolytic iron layer of the same thickness that in the experiments with CNTs. The difference in the amount of hydrogen oxidized with potassium permanganate in the absence of CNTs on a membrane and in their presence corresponded to its accumulation by nanotubes. Their hydrogen-storage capacity is calculated using the formula

$$\eta_H = (m_H/m_{CNT})100\%. \quad (2)$$

The calculations were performed under the same polarizing cathodic current in the absence of CNTs and in their presence.

The time of a single experiment was 2 h. The input side of a membrane was polarized potentiostatically under potential $E = -1.2$ V (an IPC-Pro potentiostat). The potentials were measured with respect to the saturated silver-chloride electrode and recalculated versus NHS. The average polarizing cathodic current (I_c) under the preset potential was calculated based on amount of passed electricity Q determined from the chronoamperograms (I–τ) by integration.

The amount of hydrogen absorbed by CNTs was also determined by the following method. After the exposure of the cathodically polarizable side of a membrane with the CNTs + Fe composite in a 5 M KOH solution under $E = -1.2$ V for 2 h to saturate an electrode with hydrogen, the potential was switched from −1.2 to −0.6 V, under which hydrogen oxidation in the same solution occurred. It was manifested by the current peak in the chronoamperogram (CA). The hydrogen-oxidation potential was preestablished from voltamperograms. Amount of electricity Q consumed by the hydrogen oxidation was determines from the CA by integrating the hydrogen-oxidation current peaks. A similar experiment without CNTs was performed with a membrane coated by an iron layer of the same weight as that in the CNTs + Fe composite.

Voltamperograms were recorded in the range of −1.2 to +0.2 in the straight and reverse directions at the scanning speed of 0.66 mV/s.

The electrochemical impedance of the considered electrodes was studied in the frequency range of ($\omega/2\pi$) 10 kHz to 50 mHz with an AC voltage amplitude of 10 mV using a Solartron electrochemical ana-

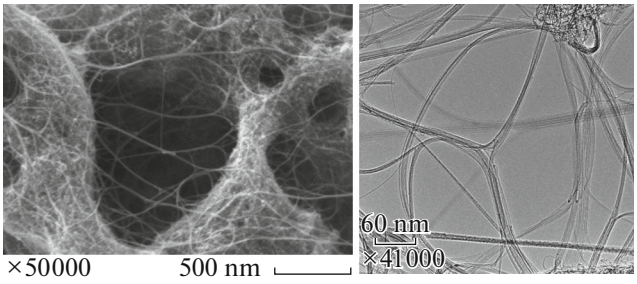

Fig. 1. SEM and PEM images of double- and triple-walled CNTs.

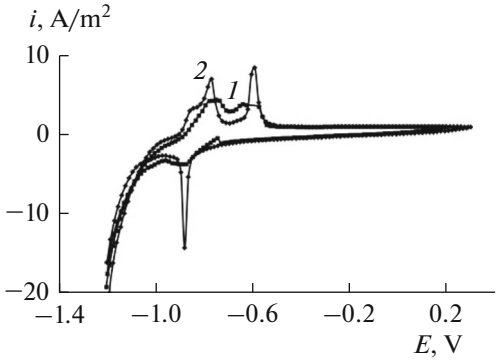

Fig. 2. VAs recorded on a steel membrane with 48 μg of CNTs encapsulated by an electrolytic iron layer in a 5.0 M KOH solution: (*1*) steel coated with an iron layer of the thickness of 10 nm; (*2*) steel with double- and triple-walled carbon nanotubes deposited on the surface and encapsulated by an electrolytic iron layer with a thickness of 10 nm.

lyzer (United Kingdom), in accordance with the technique described in [7].

The SEM and PEM images of double- and triple-walled CNTs are given in Fig. 1. In Fig. 2, once can see the voltamperograms recorded at the potential scanning speed of 0.66 mV/s from the cathode region to the anode one back on a steel membrane with deposited 48 μg of CNTs encapsulated by iron after the exposure for 3 h under the potential of −1.2 V. The current peak in the cathode region under $E = -0.9$ V corresponds to the saturation of an electrode with hydrogen. In the voltamperograms, there are two peaks in the anode region at −0.75 and −0.6 V, where the oxidation of hydrogen absorbed by nanotubes is possible because the equilibrium potential HRR in a 5 M KOH solution is more negative, which can be seen from the following calculation:

$$E_{eq} = -0.059\ \text{pH}.$$

With consideration of pH of 14.24 in a 5 M KOH solution,

$$E_{eq} = 0.059 \times 14.24 = -0.84\ \text{V}.$$

The oxidation of accumulated hydrogen occurs with some overvoltage.

In the absence of CNTs on a membrane, there are also peaks in the anode region of the voltamperogram, although they are less expressed. Apparently, newly precipitated iron absorbs hydrogen, which oxidizes in the anode region under the same potentials. However, more expressed peaks in the presence of CNTs indicate the hydrogen accumulation by carbon nanotubes. The amount of electricity corresponding to the oxidation of hydrogen absorbed by CNTs (Q_{CNT}) was determined based on the difference $Q_{CNT} = Q_{CNT + Fe} - Q_{Fe}$, where $Q_{CNT + Fe}$ is the total amount of electricity consumed by the oxidation of hydrogen in the CNT + Fe composite and Q_{Fe} is the amount of electricity consumed by the oxidation of hydrogen absorbed by iron. The hydrogen content per CNT weight unit was calculated using the following formula:

$$\eta_H = Q_{CNT} E_H / (F m_{CNT}). \quad (3)$$

Though two hydrogen oxidation peaks are observed in the current–voltage curves in the anode region (−0.75 and −0.6 V) and the potential was switched from −1.2 V, under which saturation of the composite with electrolytic hydrogen occurred, to $E = -0.6$ V, it can be suggested that, under this potential, all of the hydrogen accumulated by nanotubes oxidizes. In Table 1, the data on the hydrogen-storage capacity of nanotubes according to the electrochemical diffusion studies in a Devanathan cell and switching the membrane polarization with CNTs layer encapsulated by an iron from the cathodic potential of −1.2 V (after the double exposure for 1 h) to the hydrogen oxidation potential of (−0.6 V) and the subsequent determination of the amount of electricity corresponding to the oxidation of absorbed hydrogen are shown. As can be seen, there is a tendency toward an increase in the storage capacity under a decrease in the amount of CNTs on a membrane (or under an increase in the m_{Fe}/m_{CNT} ratio), which, apparently, indicates the existence of an optimal value that makes it possible to most effectively use CNTs.

The results of the parallel experiments, each one being the averaged value of the triple measurements performed under the identical conditions, shown in Table 1 in some cases differ significantly in terms of the absolute η_H value. Such a difference in the experi-

Table 1. Experimental data on hydrogen absorption by CNTs in 5.0 M KOH under $E = -1.2$ V

m_{MWCNT} on a membrane, mg	0.032	0.048	0.096
η_H, % (diffusion technique)	25; 19	14.5	5.7; 5.4
η_H, % (switching of polarization)	9.0; 12.1	8.1	4.2

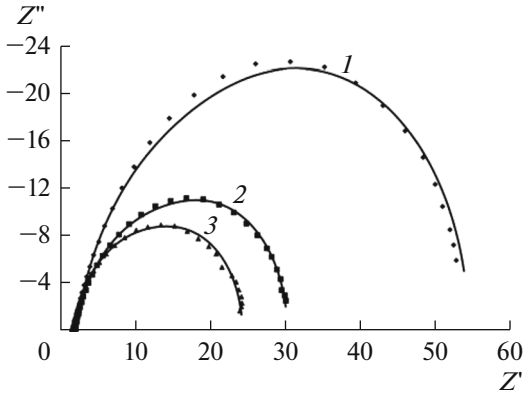

Fig. 3. Nyquist plots for a membrane coated with CNTs (96 μg) and encapsulated by an electrolytic iron layer with a thickness of 10 nm under $E = -1.2$ V in a 5 M alkaline solution. Points correspond to the experimental data; curves correspond to the adjustment in accordance with the equivalent circuit. Numbers at curves are cycle numbers. Z' (Ω cm^2) is the real component of the impedance; Z'' (Ω cm^2) is the imaginary component of the impedance.

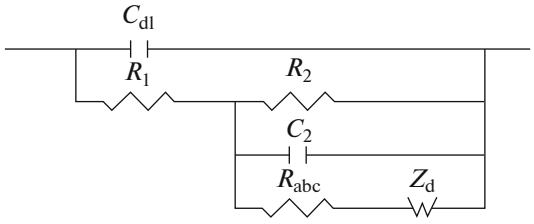

Fig. 4. Equivalent electrical circuit for HRR + HAR.

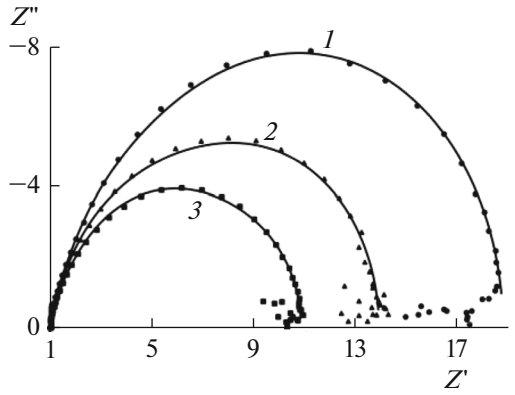

Fig. 5. Nyquist plots for a membrane encapsulated by an iron layer of the thickness of 10 nm in the absence of CNTs under $E = -1.2$ V in a 5 M alkaline solution. Points correspond to the experimental data; curves correspond to the adjustment in accordance with the equivalent circuit. Numbers by curves are cycle numbers. Z' (Ω cm^2) is the real component of the impedance; Z'' (Ω cm^2) is the imaginary component of the impedance.

mental data cannot be explained even by the change in the conditions of the discharge of proton donors and the hydrogen sorption and other characteristics of the experiment.

Such a picture is specific for nanoobjects. According to [8], if a system is far from the equilibrium, it is characterized by the absence of thermodynamic stability of the processes. Far from the region that is near the equilibrium, multiple possible states and, thus, the unpredictability must be considered. The loss of stability is explained by the theory of stability of non-linear differential equations, which, undoubtedly, describe the processes with the participation of nanoparticles when their effective size, which can also change in time, becomes the thermodynamic parameter [9]. The main ratios characterizing the loss of stability and the ambiguity of the solutions including the bifurcation as branching of solutions for such equations are used in this case.

The impedance hodographs were recorded on a membrane with double- and triple-walled CNTs deposited all over the surface in the amount of 96 μg encapsulated by an electrolytic iron layer in a 5 M KOH solution under $E = -1.2$ V (Fig. 3) immediately under the potential application (the first cycle) and after the exposure under this potential for 0.5 h (the second cycle) and then 1 h (the third cycle). The similar measurements were performed with an iron membrane in the absence of CNTs.

The processing of the impedance spectra was performed as in [7] in accordance with the equivalent circuit shown in Fig. 4, which corresponds to the molecular-hydrogen release reaction (HRR) in the presence of the hydrogen absorption (HAR) [10, 11]. According to [11], the hydrogen absorption by an electrode occurs through the adsorbed state. R_1, R_2, and C_2 are the elements of the Faraday impedance HRR; R_{abs} is the absorption reaction resistance, i.e., the phases of the H_{ads} transition to the near-surface position; and Z_d is the impedance of the diffusion of hydrogen atoms in a membrane. The diffusion impedance in the general form is expressed by the following relation:

$$Z_d = R_d \frac{\tanh\left(j\omega\tau_d\right)^{p_d}}{\left(j\omega\tau_d\right)^{p_d}},$$

where R_d is the diffusion resistance and τ_d is the characteristic time of diffusion ($\tau_d = d^2/D$, d is the membrane thickness, and D is the diffusion coefficient). The fixed value $p_d = 0.5$ was used.

The impedance hodographs recorded on a membrane coated by an electrolytic iron layer of the thickness of 10 nm in the absence of CNTs under $E = -1.2$ V in a 5 M alkaline solution are shown in Fig. 5. The numerical values of elements of the equivalent circuit for hodographs shown in Figs. 3 and 5 are shown in Tables 2 and 3.

The calculation of diffusion coefficient D of hydrogen in a steel membrane coated with an iron layer (10 nm) based on the characteristic time $\tau_d = 11.9$–17.3 s in the absence of CNTs on a membrane (see Table 3) was performed in accordance with the following for-

Table 2. Numerical values of the equivalent circuit elements for a steel membrane coated with CNTs (96 μg) encapsulated by an iron layer of the thickness of 10 nm under $E = -1.2$ V in a 5 M KOH solution

Element	1st cycle	2nd cycle	3rd cycle
R_s, Ω cm^2	1.445	1.458	1.405
C_{dl}, μF/cm^2	0.00030458	0.00052569	0.00032545
R_1, Ω cm^2	2.854	2.320	1.879
R_2, Ω cm^2	11.32	20.32	19.35
C_2, μF/cm^2	0.00020154	0.00039687	0.00023548
R_{abs}, Ω cm^2	30.66	28.63	23.94
R_d, Ω cm^2	290.32	215.65	159.34
τ_d, s	60.3278	53.25	50.96
p_d	0.5	0.5	0.5
χ^2/sum	0.0004872/0.0801	0.0004524/0.03254	0.0003652/0.03254

Table 3. Numerical values of the equivalent circuit elements for a steel membrane coated with an iron layer of the thickness of 10 nm under $E = -1.2$ V in a 5 M KOH solution

Element	1st cycle	2nd cycle	3rd cycle
R_s, Ω cm^2	0.98406 (N/A)	1.001 (N/A)	1.041 (N/A)
C_{dl}, μF/cm^2	6.1×10^{-4} (2.23)*	5.9×10^{-4} (8.873)	5.9×10^{-4} (19.873)
R_1, Ω cm^2	2.9 (15.676)	2.986 (2.88388)	2.986 (2.8858)
R_2, Ω cm^2	19.54 (2.647)	11.73 (13.955)	6.978 (15.107)
C_2, μF/cm^2	3.7×10^{-4} (19.47)	3.5×10^{-4} (25.11)	5.6×10^{-4} (36.581)
R_{abs}, Ω cm^2	7.1 (36.854)	6.4 (53.285)	7.6 (6.8628)
R_D, Ω cm^2	119.3 (15.481)	82.0 (6.3688)	63.32 (8.3735)
τ_d, s	11.88 (16.134)	12.81 (5.5743)	17.27 (5.63588)
p_d	0.5 (N/A)	0.5 (N/A)	0.5 (N/A)
χ^2/sum	0.00022026/0.01718	0.0003378/0.026348	0.00042888/0.033453

* Numbers in parentheses are the parameter errors in %; sum is the sum of quadratic deviations.

mula: $\tau = d^2/D$, where D is the diffusion coefficient of hydrogen in a membrane, which is $D = (5.2–7.5) \times 10^{-5}$ cm^2/s; this agrees satisfactorily with the reference data for D in iron at room temperature (7.8×10^{-5}–8.3×10^{-5} cm^2/s at 22–25°C). Thus, the obtained data can be considered rather reliable.

The measurement of hydrogen diffusion through a membrane with CNTs deposited on it showed that a part of hydrogen is retained by nanotubes, i.e., double- and triple-walled nanotubes can act a hydrogen traps as MWCNTs in [7]. In [12], the hydrogen capture by traps is studied and it is concluded that the impedance curve for the pure diffusion and that for the hydrogen diffusion with its capture by traps are similar. The presence of traps leads to the decrease in the effective hydrogen-diffusion coefficient in the solid phase, thus, the hydrogen capture by traps can be expressed in the increase in the characteristic time of diffusion. It follows from Tables 2 and 3 that the $\tau_{d, CNT}/\tau_{d, 0}$ ratio ($\tau_{d, 0}$ and $\tau_{d, CNT}$ are the times of diffusion in the absence and in the presence of CNTs, respectively) is 5.07, 4.15, and 2.95 in the first, second, and third cycles, respectively, i.e., the impedance data in the case of double- and triple-walled CNTs also indicate the presence of the hydrogen capture by carbon nanotubes deposited on the surface of a membrane electrode.

Hence, the impedance spectroscopy data qualitatively confirm the results on the hydrogen accumulation by the studied CNTs according to electrochemical diffusion and cyclic voltamperometry.

CONCLUSIONS

The accumulation of electrolytic hydrogen by double-triple-walled carbon nanotubes encapsulated by a thin electrolytic iron layer in a 5 M KOH solution was studied by electrochemical diffusion, cyclic voltamperometry, and impedance spectroscopy. The research data qualitatively agree with the previous results for similar composites with MWCNTs. The hydrogen-storage capacity of nanotubes depends on the Fe–CNTs weight ratio in the composite decreasing under the increase in the latter.

The observed noticeable variance of the experimental data is caused by the nature of nanoobjects and is, apparently, related to the change in the effective size of nanoparticles, which is their thermodynamic parameter, in time.

ACKNOWLEDGMENTS

This work was supported using the equipment of the Nanochemistry and Ecology Center for Collective Use at Derzhavin Tambov State University.

REFERENCES

1. V. Gayathri, N. R. Devi, and R. Geetha, "Hydrogen storage in coiled carbon nanotubes," Int. J. Hydrogen Energy **35**, 1313–1320 (2010).
2. G. E. Ioannatos and X. E. Verykios, "H_2 storage on single- and multi-walled carbon nanotubes," Int. J. Hydrogen Energy **35**, 22–28 (2010).
3. L. E. Tsygankova, "Carbon nanotubes as hydrogen accumulator," Aktual. Innovatsyonnye Issled.: Nauka Prakt., No. 1, (2011).
4. S. Iijima, "Helical microtubules of grafitic carbon," Nature **354**, 56–58 (1991).
5. L. N. Solodkova, B. F. Lyakhov, A. G. Lipson, and A. Yu. Tsivadze, "Electrochemical sorption of hydrogen in single-wall carbon nanotubes encapsulated in palladium," Prot. Met. Phys. Chem. Surf. **46**, 524–527 (2010).
6. L. E. Tsygankova, V. I. Vigdorovich, and A. A. Zvereva, "Surface state of carbon materials and accumulation of hydrogen in multiwalled carbon nanotubes," Prot. Met. Phys. Chem. Surf. **49**, 669–676 (2013).
7. L. E. Tsygankova, V. I. Vigdorovich, A. A. Zvereva, and V. I. Kichigin, "A study of hydrogen accumulation in multiwall carbon nanotubes by electrochemical techniques," Prot. Met. Phys. Chem. Surf. **52**, 211–217 (2016).
8. I. D. Kondepudi and I. Prigogine, *Modern Thermodynamics: From Heat Engines to Dissipative Structures* (Wiley, New York, 1998; Mir, Moscow, 2009).
9. V. I. Vigdorovich and L. E. Tsygankova, "Thermodynamics of microstructure materials," Prot. Met. Phys. Chem. Surf. **48** (5), 501–507 (2012).
10. C. Gabrielli, P. P. Grand, A. Lasia, and H. Perrot, "Investigation of hydrogen adsorption-absorption into thin palladium films. I. Theory," J. Electrochem. Soc. **151** (11), A1925–A1936 (2004).
11. V. I. Kichigin, I. N. Sherstobitova, and A. B. Shein, *Impedance of Electrochemical and Corrosion Systems* (Perm State Univ., Perm, 2009) [in Russian].
12. J.-P. Diard and C. Montella, "Diffusion-trapping impedance under restricted linear diffusion conditions," J. Electroanal. Chem. **557**, 19–36 (2003).

Translated by E. Petrova